

PMU Data Characterization and Application to Stability Monitoring

A. P. Sakis Meliopoulos, George J. Cokkinides
School of Electrical and Computer Engineering
Georgia Institute of Technology
Atlanta, Georgia 30332 – 0250

O. Wasynczuk E. Coyle M. Bell
School of Electrical and Computer Engineering
Purdue University
West Lafayette, Indiana 47907

C. Hoffmann C. Nita-Rotaru
Computer Science Department
Purdue University
West Lafayette, Indiana 47907

T. Downar L. Tsoukalas R. Gao
School of Nuclear Engineering
Purdue University
West Lafayette, Indiana 47907

Abstract: *This paper provides a methodology to characterize the accuracy of PMU data (GPS-synchronized) and the applicability of this data for monitoring system stability. GPS-synchronized equipment (PMUs) is in general higher precision equipment as compared to typical SCADA systems. Conceptually, PMU data are time tagged with precision better than 1 microsecond and magnitude accuracy that is better than 0.1%. This potential performance is not achieved in an actual field installation due to errors from instrumentation channels and system imbalances. Presently, PMU data precision from substation installed devices is practically unknown. On the other hand, specific applications of PMU data require specific accuracy of data. Applications vary from simple system monitoring to wide area protection and control to voltage instability prediction and transient stability monitoring. The paper focuses on the last application, i.e. transient stability monitoring. We propose an approach that is based on the energy functions (Lyapunov indirect method). Specifically, we provide a methodology for determining the required data accuracy for the reliable real time estimation of the energy function. When the data meet these requirements, the estimated energy function can be visualized and animated providing a powerful visual tool for observing the transient stability or instability of the system.*

Index Terms— PMU, GPS-synchronization, Data Accuracy, Energy Function, Transient Stability.

Glossary

GPS: Global Positioning System

PMU: Phasor Measurement Unit
CT: Current Transformer
VT: Voltage Transformer
CCVT : Capacitor Coupled Voltage Transformer

Introduction

Monitoring the operating state of the system and assessing its stability in real time has been recognized as a task of paramount importance and a tool to avert blackouts. It is also recognized that when real time data are used to derive the real time dynamic model of the system, it is possible to predict the behavior of the system and therefore will enable preventive action. This paper presents preliminary work in this area. The paper is focused on the utilization of the available data for extracting a real time dynamic model. The procedures described are decentralized, i.e. the data are utilized at each substation/generating substation of the system and they are globally valid. It is shown that if GPS-synchronized data are available at each substation this is possible. We describe the technology of GPS-synchronized measurements first. The utilization of this data for extracting the real time dynamic model is described. This model is used to predict system stability.

An important issue is the accuracy of the available data. Specifically, GPS-synchronized equipment (PMUs) is in general higher precision equipment as compared to typical SCADA systems. Conceptually, PMUs provide measurements that are time tagged with precision better than 1 microsecond and magnitude accuracy that is better than 0.1%. This

potential performance is not achieved in an actual field installation because of two reasons: (a) different vendors use different design approaches that result in variable performance among vendors, for example use of multiplexing among channels or variable time latencies among manufacturers result in timing errors much greater than one microsecond, and (b) GPS-synchronized equipment receives inputs from instrument transformers, control cables, attenuators, etc. which introduce magnitude and phase errors that are much greater than the precision of PMUs. For example, many utilities may use CCVTs for instrument transformers. We refer to the errors introduced by instrument transformers, control cables, attenuators, etc. as the instrumentation channel error. The end result is that “raw” phasor data from different vendors cannot be used as highly accurate data.

GPS-synchronized data offer the possibility of dramatically improved applications, such as real time monitoring of the system, improved state estimation, direct state measurement, precise disturbance monitoring, transient instability prediction, wide area protection and control, voltage instability prediction and many others. For proper functioning of each one of these applications, a certain precision of the data is required. The table below illustrates the data precision required for different applications in a qualitative way.

Application	Required Data Accuracy
Steady State Monitoring	Low
Disturbance Monitoring	Moderate
State Measurement	High
State Estimation	High
Wide Area Protection	Moderate
Transient Instability Monitoring	High

Conceptually, the overall precision issue can be resolved with sophisticated calibration methods. This approach is quite expensive and faces difficult technical problems. It is extremely difficult to calibrate instrument transformers and the overall instrumentation channel in the field. Laboratory calibration of instrument transformers is possible but a very expensive proposition if all instrument transformers need to be calibrated. In the early 90's the authors directed a research project in which we developed calibration procedures for selected NYPA's high voltage instrument transformers [9]. From the practical point of view, this approach is an economic impossibility. An alternative approach is to utilize appropriate filtering techniques for the purpose of correcting the magnitude and phase errors, assuming that the characteristics of the various GPS-synchronized equipment are known and the instrumentation feeding this equipment is also known.

We propose a viable and practical approach to correct for errors from instrumentation, system imbalances and data acquisition systems. It is important also to note that this process is integrated with the process of estimating the real time dynamic model of the system. The overall approach is

based on an estimation process at the generating substation/substation level for correcting these errors. Specifically, we propose a methodology that performs as a “super-calibrator”. This method and computational procedure may reside at the substation, and it can operate on the streaming data. The method can be implemented using standard communication protocols, such as the IEC 61850. The process is fast and therefore it can be applied on real time data on a continuous basis introducing only minor time latencies. The proposed methodology is based on a statistical estimation methodology that requires (a) the characteristics of GPS-synchronized equipment (PMUs), (b) a detailed model of the substation including the model of the instrumentation, and (c) the detailed model of generating units.. Subsequent paragraphs present the models of the GPS-synchronized equipment as well as the substation and generating unit(s) model with the instrumentation channels.

The overarching long-term objective of our work is to achieve a multi-scale symbiotic relationship between measurement and simulation. The work described here is part of a larger project to investigate fundamentally new algorithmic and sensing methods which can be introduced at multiple spatial scales to achieve real time simulation. We will investigate the coupling of well established power flow simulation techniques with computationally less intensive methods such as neural networks [12] to perform large scale real time applications which incorporate dynamic feedback from a network of grid monitoring sensors. This work will be based on the paradigm of Dynamic Data Driven Applications Systems (DDDAS) [13] to dynamically inject real-time grid data into power grid simulations as they execute. This should enhance the predictive capabilities of existing transient power grid stability simulations to impact the prevention of large-scale grid failures. The incorporation of real-time data will also enhance the ability to gather all the data contributing to a major blackout and to analyze and identify the current limitations of the processes used to control and operate the grid. The work described in this paper is an important first step towards this goal.

Method Description

The methodology is based on a detailed, integrated model of the power system, instrumentation channel and data acquisition system. The power system model is a detailed three-phase, breaker oriented model and includes the substation, the generating units and the interconnected transmission lines. The instrumentation channel model includes instrument transformers, control cables, attenuators, burdens, and A/D converters. The modeling approach is physically based, i.e. each model is represented with the exact construction geometry and the electrical parameters are extracted with appropriate computational procedures. As the data stream, each set of data at a specific time tag is processed via a general state estimation process that “fits” the data to the

integrated model. The procedure provides the best estimate of the data as well as performance metrics of the estimation process. The most important metric is the expected value of the error of the estimates. The best estimate of the data is used to regenerate the streaming data flow (this data is now filtered). The overall approach is illustrated in Figure 1.

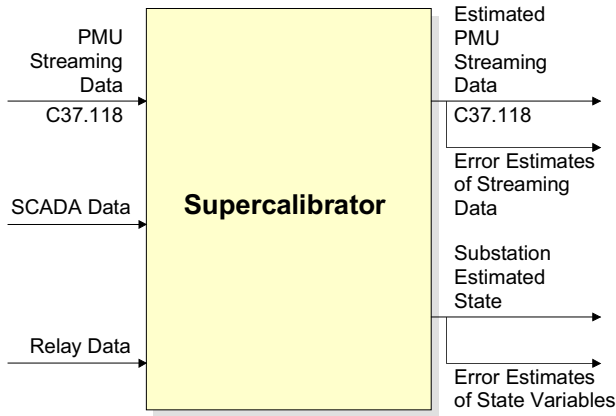


Figure 1. Inputs and Outputs of the Super-Calibrator

Generating Substation State Estimation

Instrumentation and other measurement data errors are filtered with state estimation methods. We describe a dynamic state estimation method. To introduce the method, consider the single line diagram of the substation of Figure 2. The state of the system is defined as the minimum number of independent variables that completely define the state of the system. For the substation of Figure 1 the state of the system consists of: (a) the phasor voltages of phase A, B and C of the two buses (transformer high side and low side), and (b) the generator speed (frequency) and acceleration (frequency rate of change). In summary, the state of the generating substation of Figure 2 is defined in terms of 6 complex variables and two real variables.

The number of measurements for this system from GPS-synchronized equipment, relays and standard SCADA system is quite large. Typically, the direct voltage measurements alone will have a redundancy of two to three, i.e. two to three times the number of voltage states. The available current measurements will generate a much larger redundancy considering that there will be CTs at each breaker, transformer, reactors, etc. For the system of Figure 2, and with a typical instrumentation, there will be more than 120 measurement data. This represents a redundancy level of 850%.

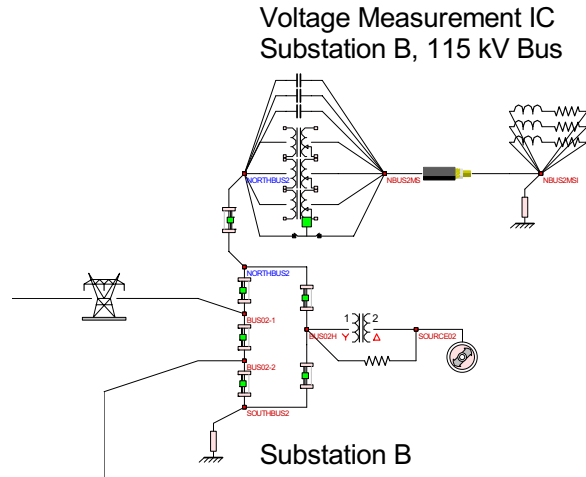


Figure 2. Breaker-Oriented Three-Phase Generating Substation Model

The state of the system is defined as the phasors of the phase voltages at each bus and the generator speed (frequency) and acceleration (rate of change of frequency) for each generating unit. A bus k will have three to five nodes, phases A, B and C, possibly a neutral and possibly a ground node. Under normal conditions the voltage at the neutral or ground will be very small and it will be assumed to be zero for this application. The state of the system at this bus is the node voltage phasors. We will use the following symbols.

$$\begin{aligned} \tilde{V}_{k,A} &= \tilde{V}_{k,A} = V_{k,A,r} + jV_{k,A,i} \\ \tilde{V}_{k,B} &= \tilde{V}_{k,B} = V_{k,B,r} + jV_{k,B,i} \\ \tilde{V}_{k,C} &= \tilde{V}_{k,C} = V_{k,C,r} + jV_{k,C,i} \end{aligned}$$

$$f_{gi}, \text{ and } \frac{df_{gi}}{dt}$$

And all internal state variables for the generators (see Appendix A).

The state of the system is defined by the vector x which contains all above real variables.

The measurements can be GPS-synchronized measurements, relay data or usual SCADA data. A typical list of measurement data is given in Table 1. The measurements are assumed to have an error that is statistically described with the meter accuracy.

Table 1. List of Measurements

Phasor Measurements	Non-Synchronized Measurements
Description	Description
Voltage Phasor, \tilde{V}	Voltage Magnitude, V
Current Phasor, \tilde{I}	Real Power Flow, P_f
Current Inj. Phasor, \tilde{I}_{inj}	Reactive Power Flow, Q_f
Frequency	Real Power Injection, P_{inj}
Rate of frequency change	Reactive Power Inj., Q_{inj}

Each measurement is related to the state of the system via a function. Since the instrumentation channel introduces substantial error, we include the instrumentation channel model in the overall model of each measurement. Specifically, consider measurement j , represented with the variable y_j . This measurement can be a GPS-synchronized measurement (phasor) or a non-synchronized measurement (scalar). Consider the instrumentation channel model and the transfer function of the instrumentation channel for this measurement defined with the function $g_j(f)$, f : frequency. Then the measurement on the power system side, z_j , is:

$$z_j = \frac{y_j}{g_j(f = 60\text{Hz})}$$

Each measurement, z_j , can be expressed as a function of the substation state. We provide here examples of measurements and the mathematical expression that relates the measurement to the state.

Phasor measurement of voltage: Consider the phasor measurement of the phase A voltage of BUS161. The model for this measurement is:

$$z_{r1} + jz_{i1} = G_1 e^{j\alpha_1} (\tilde{V}_{1,a} - \tilde{V}_{1,n})$$

Phasor measurement of current: Consider the phasor measurement of the phase A current of line L1. The model for this measurement is:

$$z_{r2} + jz_{i2} = G_2 e^{j\alpha_2} (\tilde{I}_{L1,a})$$

The model of the instrumentation channel is obtained from the physical characteristics of the instrument transformers, control cable, termination impedances, A/D conversion devices, etc. The physical structure of instrumentation channels is depicted in Figure 3.

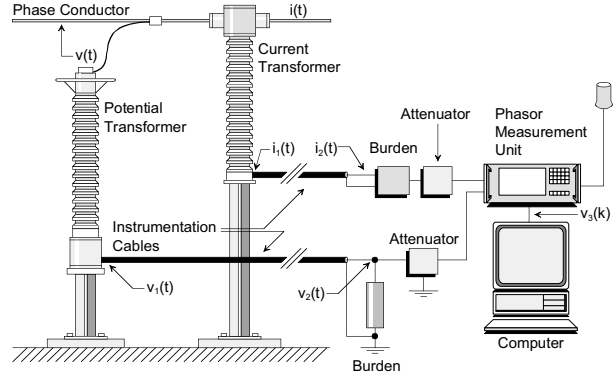


Figure 3. Typical Instrumentation Channel for PMU/Relay/IED Data Collection

In addition, since it is not practical to measure the generator internal states, a number of pseudomeasurements are generated and added to the measurement set. The pseudomeasurements are described in Appendix B.

Given a set of measurements, the state of the system is computed via the well known least square approach. Specifically, let z_i be a measurement and $h_i(x)$ be the function that relates the quantity of the measurement to the state of the system. The state is computed from the solution of the following optimization problem.

$$\text{Min } J = \sum_i \left(\frac{z_i - h_i(x)}{\sigma_i} \right)^2$$

where σ_i is the meter accuracy.

Solution methods for above problem are well known. In subsequent paragraphs, the models of the measurements and the details of the hybrid state estimator are described.

Description of Measurement Model

This section presents the overall measurement model. This model expresses each measurement as a function of the system state. By appropriate selection of the power component models, the relationship of the measurements to the states is linear or at most quadratic. The measurement set consists of the actual measurements (for example those that are defined in table 1) and a set of pseudo measurements (see Appendix B). The power system model consists of algebraic equations as well as dynamic equations; see for example the generator model in Appendix A. We convert the dynamical equations into algebraic by use of the quadratic integration method. The end result is that the power system model consists of algebraic equations which are a combination of complex and real equations. The state of the system has been defined in the previous section. The model equations, i.e. the equations that relate the state to the measurements are given below.

$$z_{V,k,A} = g_{V,k,A} (60\text{Hz}) \tilde{V}_{k,A}$$

$$z_{V,k,A} = g_{V,k,A} (60\text{Hz}) \tilde{V}_{k,A}$$

$$z_{V,k,A} = g_{V,k,A} (60\text{Hz}) \tilde{V}_{k,A}$$

$$\tilde{I}_{d1,k,A} = C_{d1,k,A}^T x, \text{ similarly for phases B and C.}$$

$$V_{k,A} = g_{k,A} (60\text{Hz}) \sqrt{V_{k,A,r}^2 + V_{k,A,i}^2}$$

$$P_{d1,k,A} = g_{pd1,k,A} (60\text{Hz}) \text{Re} \left\{ \tilde{V}_{k,A} \left[C_{d1,k,A}^T \begin{matrix} \tilde{V}_{k,A} \\ \tilde{V}_{k,B} \\ \tilde{V}_{k,C} \\ \tilde{V}_{m,A} \\ \tilde{V}_{m,B} \\ \tilde{V}_{k,C} \end{matrix} \right]^* \right\}$$

$$Q_{d1,k,A} = g_{qd1,k,A} (60\text{Hz}) \text{Im} \left\{ \tilde{V}_{k,A} \left[C_{d1,k,A}^T \begin{matrix} \tilde{V}_{k,A} \\ \tilde{V}_{k,B} \\ \tilde{V}_{k,C} \\ \tilde{V}_{m,A} \\ \tilde{V}_{m,B} \\ \tilde{V}_{k,C} \end{matrix} \right]^* \right\}$$

To facilitate the definition and the measurements and to devise a scheme for interfacing with the three-phase quadratized power system model, each measurement is defined with the following set:

$$S_{meas} = \{ m_{type} \quad n_{device} \quad n_{bus} \quad n_{phase} \}$$

where:

m_{type} : measurement type defined as in Table 3.1

n_{device} : power device ID, plus manufacturer and IED (relay, RTU, etc.) ID

n_{bus} : bus name

n_{phase} : measurement phase, A, B or C

The above set allows complete correspondence between measurement and system state.

Description of the Hybrid Three-Phase State Estimator

The hybrid three-phase state estimator uses standard SCADA data and synchronized data together with a full three-phase system model to estimate the system state. The measurement data has been discussed in the previous section. The measurements are assumed to have an error that is statistically described with the meter accuracy. As an example, the measurement of a phase voltage phasor has the following mathematical model.

$$z_{V,k,A} = g_{V,k,A} (60\text{Hz}) \tilde{V}_{k,A} + \tilde{\eta}_{V,k,A}$$

where $\tilde{\eta}_{V,k,A}$ is the measurement error.

In general, the measurements will have a general form as follows:

GPS-synchronized measurements:

$$z_s = H_s x + \eta_s$$

Non-synchronized measurements

$$z_n = H_n x + \{x^T Q_i x\} + \eta_n$$

Note that the GPS-synchronized measurements are linear with respect to the substation state, while the non-synchronized measurements are quadratic with respect to the substation state.

Now, the state estimation problem is formulated as follows:

$$\text{Min } J = \sum_{v \in \text{phasor}} \frac{\tilde{\eta}_v^* \tilde{\eta}_v}{\sigma_v^2} + \sum_{v \in \text{non-syn}} \frac{\eta_v \eta_v}{\sigma_v^2}$$

It is noted that if all measurements are synchronized the state estimation problem becomes linear and the solution is obtained directly. In the presence of the non-synchronized measurements and in terms of above formulation, the problem is quadratic, consistent with the quadratized power flow. Specifically, using the quadratic formulation and the separation of the measurements into phasor and non-synchronized measurements as has been indicated earlier and repeating these equations:

$$z_s = H_s x + \eta_s$$

$$z_n = H_n x + \{x^T Q_i x\} + \eta_n$$

In above equations, the subscript s indicates phasor measurements while the subscript n indicates non-

synchronized measurements. The best state estimate is given by:

Case 1: Phasor measurements only.

$$\hat{x} = (H_s^T W H_s)^{-1} H_s^T W z_s$$

Case 2: Phasor and non-synchronized measurements.

$$\hat{x}^{v+1} = \hat{x}^v + (H^T W H)^{-1} H^T W \begin{bmatrix} z_s - H_s \hat{x}^v \\ z_n - H_n \hat{x}^v - \{ \hat{x}^{vT} Q_i \hat{x}^v \} \end{bmatrix}$$

where:

$$W = \begin{bmatrix} W_s & 0 \\ 0 & W_n \end{bmatrix}, \quad H = \begin{bmatrix} H_s \\ H_n + H_{qn} \end{bmatrix}$$

Implementation

The proposed methodology for correcting errors from various manufacturers is being implemented into a general state estimation method. The computer model has been named the “super-calibrator”. Presently the methodology operates on the data from one substation at a time. The overall approach is shown in Figure 4.

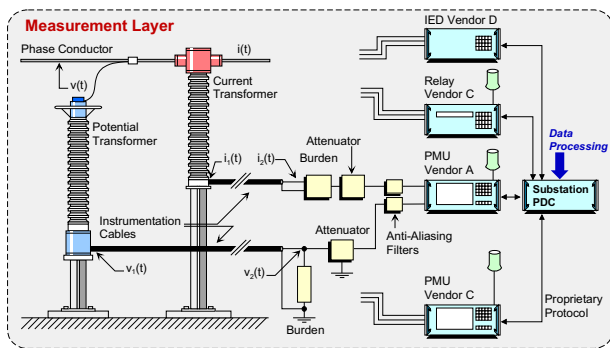


Figure 4. Conceptual Illustration of the Super-Calibrator

Application to Stability Monitoring

The output of the supercalibrator is the state of the substation including the full operating condition of the generators in case of a generating substation. Specifically, the generator speed, torque angle and acceleration is obtained from the supercalibrator. This information is enough to monitor the dynamics of the generator. Use of visualization techniques can display this information in a meaningful way to system operators. As an example, Figure 4 illustrates such a visualization. Note that the visualization shows many generators as it will be the case when the supercalibrator is implemented in all generating substations. The visualization shows the position of each generator according to its torque

angle. In addition the speed of the generator (above or below synchronous speed) is shown with arrows that are proportional to the numerical value of the speed. Note that as the information is updated from the supercalibrator, the visualization provides an animation of the motion of the system. Specifically, the supercalibrator may “run” at a rate of 60 times per second thus updating the visualization 60 times a second. This refresh speed is more than adequate to provide an excellent animation of the dynamics of the system in real time.

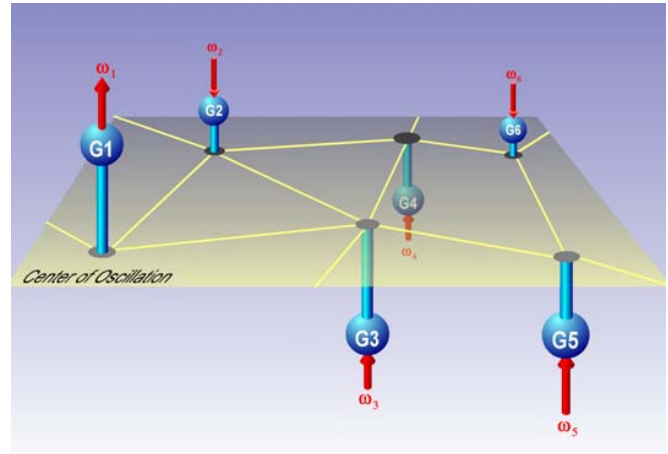


Figure 5. Visualization of Generator Real Time State

We also propose to go one step further. Specifically, we propose to use this information to predict the stability of the system. For this purpose we use the output of the supercalibrator to compute the total energy of the system. Note that the total energy of the system is defined in terms of generator torque angle and speed. At the same time the energy function can be used to determine stability boundaries. If the total energy of the system is greater than the energy at the boundaries the system motion will be unstable. This basic principle and the ability of the supercalibrator to provide the total energy of the system is used to predict the stability of the system. Presently we are working to develop appropriate visualization of the stability predictor.

Conclusions

This paper presented methodologies for filtering available data in substations (for example phasor data, relay data and SCADA data) for the purpose of extracting a real time dynamical model of the system. The real time dynamical model is used for monitoring system stability and it is capable to predict any instability that may arise.

The innovations presented here is that the entire filtering process is confined to the substation, the instrumentation channels are explicitly represented and the substation model is a breaker-oriented three-phase model and generator dynamics are included in the model. The methodology provides the means for correcting errors from instrumentation channels, phase shifts of different PMU manufacturers and

accommodates unbalanced operation and system model asymmetries.

The proposed super-calibrator provides a precise dynamic state estimator for power systems at the substation level. The estimator is ideally suited for monitoring the stability of the system as well as predicting any instability before it occurs. Applications of this concept can be extended to protection of the system with improved out of step protection and wide area special protection schemes.

Acknowledgments

The work reported in this paper has been partially supported by the NSF Grant No. 000812 and by the DoE EIPP project. This support is gratefully acknowledged.

References

- [1] A. P. Sakis Meliopoulos and George J. Cokkinides, "A Virtual Environment for Protective Relaying Evaluation and Testing", *IEEE Transactions of Power Systems*, Vol. 19, No. 1, pp. 104-111, February, 2004.
- [2] A. P. Sakis Meliopoulos and G. J. Cokkinides, "Visualization and Animation of Instrumentation Channel Effects on DFR Data Accuracy", Proceedings of the 2002 Georgia Tech Fault and Disturbance Analysis Conference, Atlanta, Georgia, April 29-30, 2002
- [3] T. K. Hamrita, B. S. Heck and A. P. Sakis Meliopoulos, 'On-Line Correction of Errors Introduced By Instrument Transformers In Transmission-Level Power Waveform Steady-State Measurements', *IEEE Transactions on Power Delivery*, Vol. 15, No. 4, pp 1116-1120, October 2000.
- [4] A. P. Sakis Meliopoulos and George J. Cokkinides, "Virtual Power System Laboratories: Is the Technology Ready?", *Proceedings of the 2000 IEEE/PES Summer Meeting*, Seattle, WA, July 16-20, 2000.
- [5] A. P. Sakis Meliopoulos and George J. Cokkinides, 'A Virtual Environment for Protective Relaying Evaluation and Testing', *Proceedings of the 34th Annual Hawaii International Conference on System Sciences*, p. 44 (pp. 1-6), Wailea, Maui, Hawaii, January 3-6, 2001.
- [6] A. P. Sakis Meliopoulos, George J. Cokkinides, "Visualization and Animation of Protective Relays Operation From DFR Data", *Proceedings of the 2001 Georgia Tech Fault and Disturbance Analysis Conference*, Atlanta, Georgia, April 30-May 1, 2001.
- [7] A. P. Meliopoulos and J. F. Masson, "Modeling and Analysis of URD Cable Systems," *IEEE Transactions on Power Delivery*, vol. PWRD-5, no. 2, pp. 806-815, April 1990.
- [8] G. P. Christoforidis and A. P. Sakis Meliopoulos, "Effects of Modeling on the Accuracy of Harmonic Analysis," *IEEE Transactions on Power Delivery*, vol. 5, no. 3, pp.1598-1607, July 1990.
- [9] A. P. Meliopoulos, F. Zhang, S. Zelingher, G. Stillman, G. J. Cokkinides, L. Coffeen, R. Burnett, J. McBride, 'Transmission Level Instrument Transformers and Transient Event Recorders Characterization for Harmonic Measurements,' *IEEE Transactions on Power Delivery*, Vol 8, No. 3, pp 1507-1517, July 1993.
- [10] B. Fardanesh, S. Zelingher, A. P. Sakis Meliopoulos, G. Cokkinides and Jim Ingleson, 'Multifunctional Synchronized Measurement Network', *IEEE Computer Applications in Power*, Volume 11, Number 1, pp 26-30, January 1998.
- [11] A. P. Sakis Meliopoulos and G. J. Cokkinides, "Phasor Data Accuracy Enhancement in a Multi-Vendor Environment", Proceedings of the 2005 Georgia Tech Fault and Disturbance Analysis Conference, Atlanta, Georgia, April 25-26, 2005
- [12] F. Darema, "Dynamic Data Driven Application Systems," Presentation at Purdue University, May 4, 2004, <http://www.cise.nsf.gov/eia/dddas>
- [13] L. Tsoukalas, R. Gao, T. Fieno, X. Wang, "Anticipatory Regulation of Complex Power Systems," *Proc. of European Workshop on Intelligent Forecasting, Diagnosis and Control-IFDICON 2001*, Santorini, Greece, June 2001

Biographies

A. P. Sakis Meliopoulos (M '76, SM '83, F '93) was born in Katerini, Greece, in 1949. He received the M.E. and E.E. diploma from the National Technical University of Athens, Greece, in 1972; the M.S.E.E. and Ph.D. degrees from the Georgia Institute of Technology in 1974 and 1976, respectively. In 1971, he worked for Western Electric in Atlanta, Georgia. In 1976, he joined the Faculty of Electrical Engineering, Georgia Institute of Technology, where he is presently a professor. He is active in teaching and research in the general areas of modeling, analysis, and control of power systems. He has made significant contributions to power system grounding, harmonics, and reliability assessment of power systems. He is the author of the books, *Power Systems Grounding and Transients*, Marcel Dekker, June 1988, *Lighning and Overvoltage Protection*, Section 27, Standard Handbook for Electrical Engineers, McGraw Hill, 1993, and the monograph, *Numerical Solution Methods of Algebraic Equations*, EPRI monograph series. Dr. Meliopoulos is a member of the Hellenic Society of Professional Engineering and the Sigma Xi.

Appendix A: Quadratized Two-Axes Generator Model

A two-axis quadratized synchronous generator model is developed for the representation of generators. The basic phasor diagram is presented in Figure 3. The angle of rotor position (d-axis) $\theta(t)$ and the rotor angular velocity $\omega(t)$ are defined and then the rotor angle is defined as:

$$\delta(t) = \theta(t) - \omega_s t - \frac{\pi}{2}, \quad (15)$$

where $\delta(t) + \frac{\pi}{2}$ is the angle difference between the rotor (d-axis), rotating at speed $\omega(t)$, and a synchronously rotating reference frame at speed ω_s . After quadratizing the model and introducing additional state variables, so that the differential equations are linear and the algebraic at most quadratic, the model equations in compact form are:

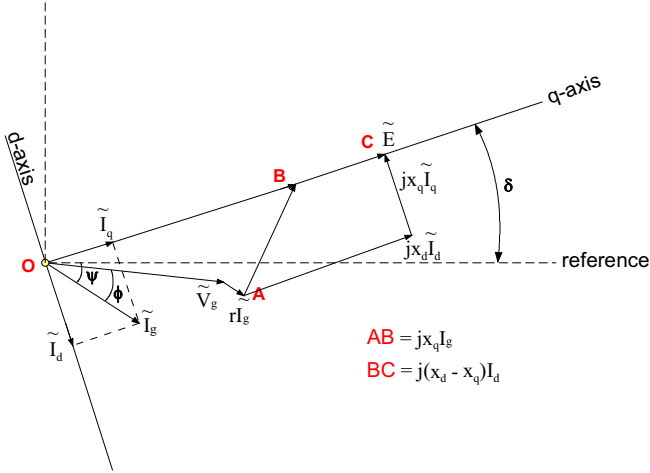


Figure A-1. Two-axis synchronous machine phasor diagram

$$\begin{aligned} \tilde{I}_g &= \tilde{I}_d + \tilde{I}_q \\ 0 &= \tilde{E} - \tilde{V}_g + r(\tilde{I}_d + \tilde{I}_q) + jx_d \tilde{I}_d + jx_q \tilde{I}_q \\ 0 &= E_r I_{dr} + E_i I_{di} \\ 0 &= E_r s(t) - E_i c(t) \\ 0 &= E_i I_{qr} - E_r I_{qi} \\ 0 &= E_r^2 + E_i^2 - E_{spec.} \\ 0 &= T_a(t) - T_m(t) + 3 \cdot z_1 (I_{dr} + I_{qr}) + 3 \cdot z_2 (I_{di} + I_{qi}) + D \cdot (\omega(t) - \omega_s) \\ 0 &= z_1 \omega(t) - E_r \\ 0 &= z_2 \omega(t) - E_i \\ 0 &= w_1(t) - c(t) \cdot \omega(t) + \omega_s c(t) \\ 0 &= w_2(t) + s(t) \cdot \omega(t) - \omega_s s(t) \\ \frac{d\delta(t)}{dt} &= \omega(t) - \omega_s \\ \frac{d\omega(t)}{dt} &= \frac{\omega_s}{2H} T_a(t) \\ \frac{ds(t)}{dt} &= w_1(t) \\ \frac{dc(t)}{dt} &= w_2(t) \end{aligned}$$

where

- \tilde{I}_g : armature current (positive direction is into the generator),
- r : armature resistance,
- x_d : direct-axis synchronous reactance,
- x_q : quadrature-axis synchronous reactance,
- \tilde{V}_g : terminal voltage,
- ω_s : synchronous speed,
- H : inertia constant of the generator,
- T_m : mechanical power supplied by a prime-mover (in p.u.),
- T_D : damping torque (p.u.), which can be approximated by $T_D = D \cdot (\omega - \omega_s)$ with D constant,

$\tilde{E} = E e^{j\delta}$ is the internal generator voltage; it is an input to the model and its magnitude is specified by an exciter system.

The state vector of the model is defined as:

$$\begin{aligned} x^T &= [x_1^T \ x_2^T], \\ \text{with} \\ x_1^T &= [\tilde{V}_g \ \tilde{E} \ \tilde{I}_d \ \tilde{I}_q], \\ x_2^T &= [T_a(t) \ z_1(t) \ z_2(t) \ w_1(t) \ w_2(t) \ \delta(t) \ \omega(t) \ s(t) \ c(t)]. \end{aligned}$$

Again the same procedure is followed here as for the motor to cast above model in the form of equation (1). Specifically, the differential equations are integrated. The resulting equations of the model to form a set of equations in the structure of equation (1).

Appendix B: Pseudomeasurements for Generator Internal States

Since it is not practical to measure the generator internal states, a number of pseudomeasurements are introduced that provide the generator internal states. The pseudomeasurements are computed from actual measurements of generator terminal voltages and currents and frequency. The computational procedure for the pseudomeasurements is described next.

First the vector A is computed:

$$\tilde{A} = \tilde{V}_g + r\tilde{I}_a + jx_q \tilde{I}_a$$

Above vector defines the location of the q-axis. Then by the geometric construction, illustrated in Figure A-1, the components of the internal states of the generator are computed. Specifically:

Currents \tilde{I}_d, \tilde{I}_q are the projections of the terminal current on the d and q axes.

The internal voltage is computed from:

$$\tilde{E} = \tilde{V}_g + r(\tilde{I}_d + \tilde{I}_q) + jx_d \tilde{I}_d + jx_q \tilde{I}_q$$

The quantities c(t) and s(t) are computed as the cosine and sine of the angle of the q-axis, etc.